J|A|C|S
ARTICLES
Published on Web 07/12/2006

Synthesis, Oxidation Behavior, Crystallization and Structure of 2′-Methylseleno Guanosine Containing RNAs

Holger Moroder,[†] Christoph Kreutz,[†] Kathrin Lang,[†] Alexander Serganov,*[,‡] and Ronald Micura*[,†]

Contribution from the Institute of Organic Chemistry, Center for Molecular Biosciences (CMBI), Leopold-Franzens University, 6020 Innsbruck, Austria, and Memorial Sloan-Kettering Cancer Center, 1275 York Ave, Box 557, New York, New York

Received March 29, 2006; E-mail: serganoa@mskcc.org; ronald.micura@uibk.ac.at

Abstract: We have recently introduced a basic concept for the combined chemical and enzymatic preparation of site-specifically modified 2′-methylseleno RNAs which represent useful derivatives for phasing of X-ray crystallographic data during their three-dimensional structure determination. Here, we introduce the first synthesis of an appropriate guanosine phosphoramidite, which complements the thus far established set of 2′-methylseleno-modified uridine, cytidine, and adenosine building blocks for solid-phase synthesis. The novel building block was readily incorporated into RNA. Importantly, it was the 2′-methylseleno-guanosine-labeled RNA that allowed us to reveal the reversible oxidation/reduction behavior of the Se moiety and thus it represents a valuable contribution to the understanding of the action of *threo*-1,4-dimercapto-2,3-butanediol (DTT) required during solid-phase synthesis, deprotection, and crystallization of selenium-containing RNA. In addition, we investigated 2′-methylseleno RNA with respect to crystallization properties. Our studies revealed that the Se modification significantly increases the range of conditions leading to crystal growth. Moreover, we determined the crystal structures of model RNA helices and showed that the Se modification can affect crystal packing interactions, thus potentially expanding the possibilities for obtaining the best crystal form.

Introduction

In nucleic acid crystallography, selenium-labeled DNA and RNA oligonucleotides have become recognized recently to represent useful derivatives for convenient phasing of X-ray crystallographic data. Pioneering work by Egli, Huang, and co-workers led to the successful MAD phasing of a short Z-form DNA duplex via phosphoroselenoate backbone modifications and of an A-form DNA duplex via 2′-methylseleno uridine modifications.[1,2] Then, our laboratory introduced advanced procedures for the preparation of 2′-methylseleno-modified RNA, site-specifically labeled at single uridines, cytidines, and adenosines (Figure 1).[3,4] Thereby, the application of *threo*-1,4-dimercapto-2,3-butanediol (DTT) during all crucial steps of RNA preparation, including the solid-phase synthesis cycle, was a major breakthrough for the high performance of the Se approach. This led to the preparation of high-purity RNAs with up to a hundred nucleotides containing site-specifically incorporated, multiple Se labels, exemplified by the adenine riboswitch aptamer domain.[4,10] Successful applications of the Se-derivatized RNAs developed in the course of this project have been reported recently and refer to the X-ray structure of the group I intron with both exons,[11] and to the recent structure

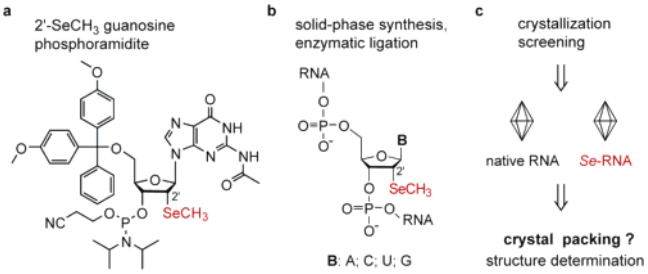

Figure 1. Se-modified RNA for X-ray crystallography. (a) The synthesis of a 2′-methylseleno-modified guanosine building block appropriate for RNA solid-phase synthesis is presented in this study. (b) 2′-Methylseleno nucleoside containing RNA is readily accessible by chemical synthesis and enzymatic ligation[3,4] and represents a valuable derivative in X-ray structure determination using advanced techniques for phase determination, such as MAD (multiwavelength anomalous dispersion), SAD (single-wavelength anomalous diffraction), or SIRAS (single isomorphous replacement with anomalous scattering).[5−9] (c) Crystallization screening and structure comparison of native vs Se-modified model RNA helices is addressed in the present study to shed light on the influence of Se modification on crystal packing interactions.

[†] Leopold-Franzens University.
[‡] Memorial Sloan-Kettering Cancer Center.

(1) Du, Q.; Carrasco, N.; Teplova, M.; Wilds, C. J.; Egli, M.; Huang, Z. *J. Am. Chem. Soc.* **2002**, *124*, 24−25.
(2) Wilds, C. J.; Pattanayek, R.; Pan, C.; Wawrzak, Z.; Egli, M. *J. Am. Chem. Soc.* **2002**, *124*, 14910−14916.
(3) Höbartner, C.; Micura, R. *J. Am. Chem. Soc.* **2004**, *126*, 1141−1149.
(4) Höbartner, C.; Rieder, R.; Kreutz, C.; Puffer, B.; Lang, K.; Polonskaia, A.; Serganov, A.; Micura, R. *J. Am. Chem. Soc.* **2005**, *127*, 12035−12045.
(5) Hendrickson, W. A.; Ogata, C. M. *Methods Enzymol.* **1997**, *276*, 494−523.
(6) Podjarny, A.; Schneider, T. R.; Cachau, R. E.; Joachimiak A. *Methods Enzymol.* **2003**, *374*, 321−341.
(7) Hendrickson, W. A. *Trends Biochem. Sci.* **2000**, *25*, 637−643.
(8) Doublié, S. *Methods Enzymol.* **1997**, *276*, 523−530.
(9) Strub, M. P.; Hoh, F.; Sanchez, J. F.; Strub, J. M.; Bock, A.; Aumelas, A.; Dumas, C. *Structure* **2003**, *11*, 1359−1367.

determination of the Diels−Alder ribozyme solved by the SAD technique via the corresponding 2′-methylseleno pyrimidine derivatives synthesized in our laboratory.[4,12]

The replacement of natural 2′-OH by 2′-methylseleno groups does not significantly interfere with the global fold of RNA if the labels are properly positioned. Provided that the 2′-methylseleno moieties reside in the covariant, double helical regions of the target fold, and provided that the 5′- and 3′-ends of the RNA comprise the same functional groups (phosphates, triphosphates, cyclophosphates, or hydroxyls) as used to crystallize the native RNA, the crystallization behavior and structure of the selenium-modified RNAs compare well with their nonlabeled counterparts.[1,4,13] Nevertheless, sugar moieties of RNA often participate in the formation of intermolecular contacts in the crystal lattice, providing valuable hydrogen bonds and van der Waals interactions.[14] In this sense, it is an absolute requirement to make all four standard nucleosides available as 2′-methylseleno building blocks for RNA solid-phase synthesis in order to not encounter any limitation in adequate positioning of the Se labels. Here, we present the first synthesis of a 2′-methylseleno guanosine phosphoramidite appropriate for RNA solid-phase synthesis and its incorporation into oligoribonucleotides. This phosphoramidite completes the set of four standard RNA nucleoside building blocks with 2′-methylseleno groups. In addition, we report on the reversible redox behavior of Se-containing RNA and on the influence of Se modifications on the crystallization and structure of model RNA helices.

Results and Discussion

Synthesis of a 2′-Methylseleno Guanosine Phosphoramidite. Our route began with the simultaneous protection of the 3′- and 5′-hydroxyl groups of commercially available 9-[β-D-arabinofuranosyl]guanine **1** using 1,3-dichloro-1,1,3,3-tetraisopropyldisiloxane ($TIPDSiCl_2$). Then, treatment of 3′,5′-protected **2** with acetic anhydride yielded a mixture of N^2,2′-*O*-diacetylated and N^2,N^2,2′-*O*-triacetylated nucleosides, **3a** and **3b**. Whereas **3a** was readily separated from **3b** by column chromatography, **3b** resisted isolation in pure form and could only be obtained together with its diacetylated counterpart **3a**. A complete separation and individual characterization of di- and triacetylated compounds, however, was achieved after protection of the guanine lactam moiety with a O^6-(4-nitrophenyl)ethyl group introduced under Mitsunobu conditions,[15] resulting in **4a** and **4b**. Protection of O^6 was mandatory since this functional group is known to be reactive toward trifluoromethanesulfonyl chloride which was required in a later step of the synthesis. For efficient large-scale synthesis, separation of the di- and triacetylated nucleoside derivatives **4a** and **4b** was not required. Starting with a mixture of them, the basic aqueous conditions of the subsequent hydrolysis step were optimized to liberate the arabinose 2′-hydroxyl group while retaining the guanine N^2 monoacetylated, representing the proper protection for the final nucleoside phosphoramidite at an early stage of the synthesis. Hydrolysis product **5** was then reacted with trifluoromethanesulfonyl chloride (Tf-Cl) to furnish nucleoside **6**, which was isolated and subsequently substituted (S_N2) by sodium methylselenide, producing key diastereoisomer **7** in high yield. Deprotection of the TIPDS moiety and simultaneous release of the O^6-(4-nitrophenyl)ethyl group proceeded straightforwardly using tetrabutylammonium fluoride (TBAF). Derivative **8** was transformed into the dimethoxytritylated compound **9**, which was phosphitylated to achieve the actual 2′-methylseleno guanosine phosphoramidite building block **10**. We point out that initial attempts to apply O^6-(*N*,*N*-diphenylcarbamoyl)[16] instead of O^6-(4-nitrophenyl)ethyl protection failed because this group was unstable and partly substituted during treatment with sodium methylselenide. Starting with 9-[β-D-arabinofuranosyl]guanine **1**, our route provides phosphoramidite **10** in a 6% overall yield in nine steps with eight chromatographic purifications; in total, 0.8 g of **10** was obtained in the course of this study (Scheme 1).

Chemical Synthesis and Deprotection of Se-Guanosine-Containing RNA. The preparation of RNA with 2′-methylseleno-modified guanosines relies on the 2′-*O*-TOM-methodology for strand assembly,[17,18] and on a previously established protocol for the synthesis of RNA with site-specific 2′-methylseleno uridine, 2′-methylseleno cytidine, and 2′-methylseleno adenosine modifications.[4] Therein, the solid-phase synthesis cycle is substantially changed from standard RNA synthesis by the insertion of a step treating the oligonucleotide chain on the solid support with *threo*-1,4-dimercapto-2,3-butanediol (DTT). The repeated exposure of the growing chain to DTT is an absolute requirement for the reliable synthesis of RNAs (>25 nt) containing multiple Se labels (>2).[4]

Along these lines, the novel phosphoramidite **10** was successfully incorporated into oligoribonucleotides with coupling yields higher than 98%, monitored via the UV-trityl assay. Cleavage from the solid support and deprotection of the 2′-methylseleno-guanosine-modified RNAs were also performed in the presence of DTT, added in millimolar amounts to the deprotection solutions of CH_3NH_2 in ethanol/H_2O and of tetrabutylammonium fluoride (TBAF) in tetrahydrofuran (THF). After deprotection, DTT was removed by size exclusion chromatography on a Sephadex G25 column. RNAs were then purified by anion-exchange chromatography under strong denaturating conditions (6 M urea, 80 °C; Figure 2). The molecular weights of the purified RNAs were confirmed by liquid chromatography (LC) electrospray-ionization (ESI) mass spectrometry (MS). Exemplarily, four RNAs containing single 2′-methylseleno guanosine labels (**11a**−**14a**) were prepared with the sequences listed in Table 1. Sequences **12** and **13** represented self-complementary 12 nt and 16 nt RNAs, each containing two isolated G•A mispairs. The structures of the corresponding unmodified duplexes were previously solved by Leonard et al. in 1994 and by Sundaralingam et al. in 1999 and are therefore considered ideal for verifying the guanosine Se approach.[19,20]

(10) Serganov, A.; Yuan, Y. R.; Pikovskaya, O.; Polonskaia, A.; Malinina, L.; Phan, A. T.; Höbartner, C.; Micura, R.; Breaker, R. R.; Patel, D. J. *Chem., Biol.* **2004**, *11*, 1729−1741.
(11) Adams, P. L.; Stahley, M. R.; Kosek, A. B.; Wang, J.; Strobel, S. A. *Nature* **2004**, *430*, 45−50.
(12) Serganov, A.; Keiper, S.; Malinina, L.; Tereshko, V.; Skripkin, E.; Höbartner, C.; Polonskaia, A.; Phan, A. T.; Wombacher, R.; Micura, R.; Dauter, Z.; Jaschke, A.; Patel, D. J. *Nat. Struct. Mol. Biol.* **2005**, *12*, 218−224.
(13) Teplova, M.; Wilds, C. J.; Wawrzak Z.; Tereshko V.; Du Q.; Carrasco, N.; Huang, Z.; Egli, M. *Biochimie* **2002**, *84*, 849−858.
(14) Shah, S. A.; Brunger, A. T. *J. Mol. Biol.* **1998**, *285*, 1577−1588.
(15) Höbartner, C.; Kreutz, C.; Flecker, E.; Ottenschläger, E.; Pils, W.; Grubmayr, K.; Micura R. *Monatsh. Chem.* **2003**, *134*, 851−873.
(16) Hirao, I.; Harada, Y.; Kimoto, M.; Mitsui, T.; Fujiwara, T.; Yokoyama, S. *J. Am. Chem. Soc.* **2004**, *126*, 13298−13305.
(17) Pitsch, S.; Weiss, P. A.; Jenny, L.; Stutz, A.; Wu, X. *Helv. Chim. Acta* **2001**, *84*, 3773−3795.
(18) Micura, R. *Angew. Chem., Int. Ed. Engl.* **2002**, *41*, 2265−2267.

Scheme 1. Synthesis of 2′-Methylseleno Guanosine Phosphoramidite **10**[a]

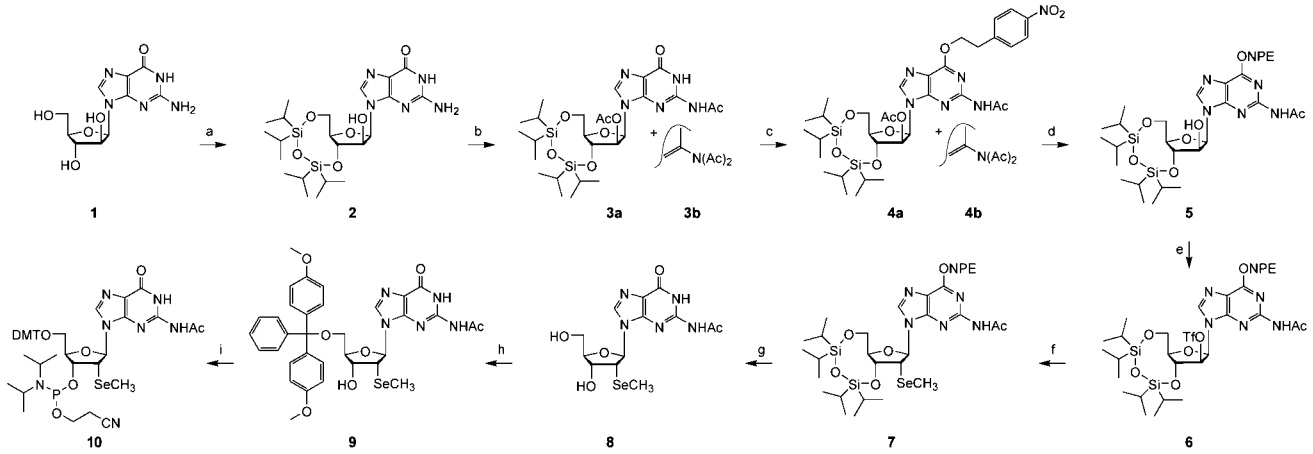

[a] (a) 1.05 equiv of $TIPDSiCl_2$, in DMF/pyridine, room temperature, 16 h, 98%; (b) 10 equiv of acetic anhydride, in DMF/pyridine, 80 °C, 16 h, 64%; (c) 1.3 equiv of NPE-OH, 1.4 equiv of PPh_3, 1.3 equiv of DIAD, in dioxane, room temperature, 3 h, 64%; (d) aqueous ammoniumhydroxide, in THF/methanol/water, 0 °C, 5 min, 57%; (e) 1.5 equiv of trifluoromethanesulfonyl chloride, 1.5 equiv of DMAP, 2.5 equiv of NEt_3, in CH_2Cl_2, 0 °C, 2 h, 69%; (f) 6 equiv of $NaBH_4$, 2 equiv of $CH_3SeSeCH_3$, in THF, 20 min, 87%; (g) 1 M TBAF, in THF, room temperature, 2.5 h, 79%; (h) 1.1 equiv of DMT-Cl, in pyridine, room temperature, 16 h, 59%; (i) 1.5 equiv of (2-cyanoethyl)-*N*,*N*-diisopropylchlorophosphoramidite, 10 equiv of $CH_3CH_2N(CH_3)_2$, in CH_2Cl_2, room temperature, 2 h, 88%; (DIAD diisopropyl azodicarboxylate, DMAP 4-(dimethylamino)-pyridine, DMT dimethoxytrityl, NPE 2-(4-nitrophenyl)ethyl, TBAF tetrabutylammonium fluoride, $TIPDSiCl_2$ 1,3-dichloro-1,1,3,3-tetraisopropyldisiloxane).

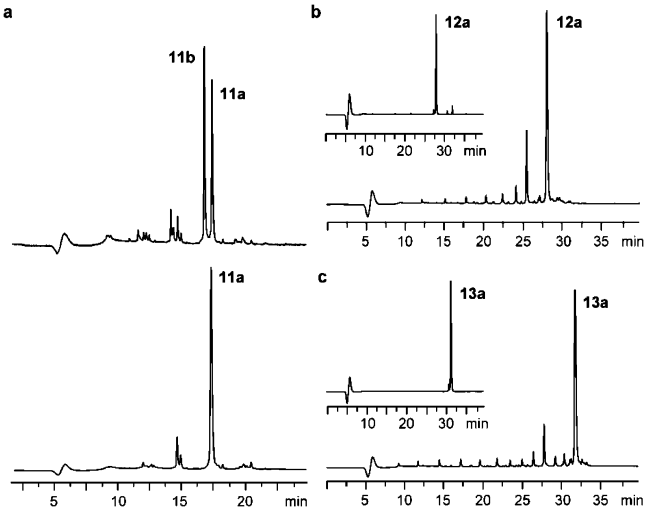

Figure 2. HPLC traces of crude, deprotected 2′-methylseleno guanosine modified RNA (anion exchange HPLC: Dionex DNAPac (4 × 250 mm), 80 °C, 1 mL/min, 0−60% B in 45 min; (A) 25 mM Tris-HCl, 6 M urea, pH 8.0; (B) same as A + 0.5 M $NaClO_4$). (a) Comparison of crude rACGG_{Se}UC **11**, prepared without (resulting in **11a** and oxidized product **11b**; top, see also Figure 3) and with (resulting in **11a** exclusively; bottom) *threo*-1,4-dimercapto-2,3-butandiol (DTT) treatment during solid-phase synthesis and deprotection. (b) and (c) Crude and purified (inset) rCG_{Se}CGAAUUAGCG **12a** and rGCAG_{Se}AGUUAAAUCUGC **13a** prepared with DTT treatment. Deprotection procedure includes three steps: (1) 150 mM DTT in EtOH/H_2O, 1−3 h, room temperature; (2) CH_3NH_2 in EtOH/H_2O, 150 mM DTT, 4−6 h, room temperature; (3) 1 M TBAF in THF, 150 mM DTT, 12−16 h, room temperature.

Sequence **14** represented a G_{Se} derivative of the 22 nt selenium-derivatized RNA/DNA hybrid that was crystallized in a ternary complex of the group I intron with both exons.[3,11]

Redox Behavior of 2′-Methylseleno-Guanosine-Containing RNAs. When the RNA hexamer **11** was prepared without the use of DTT, the HPLC profile of the crude deprotected material showed two dominating peaks, **11a** and **11b**, with a difference of 1 min in retention time (Figure 2a). Both peaks were isolated, and LC-ESI-MS analysis revealed the expected molecular weight for the slow-migrating RNA and a molecular weight of 16 mass units higher for the fast-migrating RNA. This observation gave evidence that the 2′-methylseleno group had been oxidized to the corresponding 2′-methylselenoxide group.[21] We further corroborated this hypothesis by the finding that purified **11a** was rapidly transformed into **11b** by exposure to a solution of 2,4,6-trimethylpyridine/water/acetonitrile containing 2 mM iodine. We were then able to reconvert **11b** back into **11a** upon treatment with 10 mM DTT in ethanol/water. It is remarkable that both oxidation and reduction proceeded without any side products as detected by HPLC. Moreover, the oxidation reaction seems to proceed under diastereoselective control due to observation of a single-product peak. The reversible redox behavior was also investigated and confirmed for the other Se-guanosine-containing sequences, **12**−**14** (Figure 3).

It has been noted in the literature that uniform oxidation of Se-methionine-containing protein crystals to the corresponding selenoxides and selenones results in a higher anomalous signal.[22−24] Likewise, the consistent transformation of RNA 2′-methylseleno groups into their corresponding selenoxides could be beneficial, provided the oxidation was complete, the selenoxide moieties were not structurally perturbing, and the RNA derivatives were stable enough over the period of crystallization and data collection. Our ongoing work is focused on these issues.

Crystallization of 2′-Methylseleno-Guanosine-Containing RNAs. Virtually identical structures of the Se-modified and nonmodified Diels−Alder ribozymes have proven that Se modification does not affect RNA conformation and does not necessarily change RNA packing in the crystals.[12] However, sugars often participate in the crystal packing of RNA and, if placed in contacting regions, 2′-methylseleno modifications may

(19) Leonard, G. A.; McAuley-Hecht, K. E.; Ebel, S.; Lough, D.; Brown, T.; Hunter, W. N. *Structure* **1994**, *2*, 483−494.
(20) Pan, B.; Mitra, S. N.; Sundaralingam, M. *Biochemistry* **1999**, *38*, 2826−2831.
(21) Chen, T.; Greenberg, M. M. *J. Am. Chem. Soc.* **1998**, *120*, 3815−3816.
(22) Moroder, L. *J. Peptide Sci.* **2005**, *11*, 187−214.
(23) Sharff, A. J.; Koronakis, E.; Luisi, B.; Koronaki, V. *Acta Crystallogr. D* **2000**, *56*, 785−788.
(24) Ali, M. A.; Peisach, E.; Allen, K. N.; Imperiali, B. *Proc. Natl. Acad. Sci. U.S.A.* **2004**, *101*, 12183−12188.

Table 1. RNAs Containing 2′-Methylseleno Guanosines Prepared by Solid Phase Synthesis

				isolated yield		molecular weight	
no.	sequence[a]	length (nt)	scale (μmol)	OD 260 nm	nmol	calcd (amu)	found[b] (amu)
11a	5-ACGG_{Se}UC-3	6	1	27	190	1951.2	1951.4
12a	5-CG_{Se}CGAAUUAGCG-3	12	2	78	466	3910.3	3911.4
13a	5-GCAG_{Se}AGUUAAAUCUGC-3	16	2	90	486	5182.1	5182.6
14a	5-AAGCCACACAAACC(dA)(dG)(dA)CG_{Se}GCC-3	22	1	19	92	7057.4	7056.1

[a] G_{Se}, 2′-methylseleno guanosine; dA, 2′-deoxy adenosine; dG, 2′-deoxy guanosine. [b] LC-ESI MS.

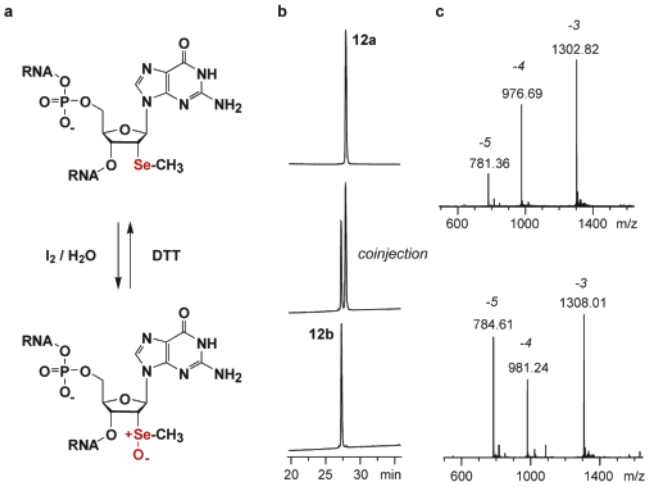

Figure 3. Redox behavior of rCG_{Se}CGAAUUAGCG **12**. (a) Chemical structures of reduced and oxidized selenium-modified RNA; reaction conditions (oxidation): 1.5 nmol of RNA, 2 mM iodine solution in H_2O/CH_3CN/*sym*-collidine; reaction conditions (reduction): 1.5 nmol of RNA, 2 mM DTT in 150 μL of H_2O. (b) HPLC traces of isolated **12a** (selenide) and **12b** (selenoxide) and co-injection (anion exchange; for conditions see Figure 2). (c) LC-ESI-MS spectra of **12a** (top; molecular weight, calcd 3911.25, found 3911.37) and **12b** (bottom; molecular weight, calcd 3927.25, found 3928.05).

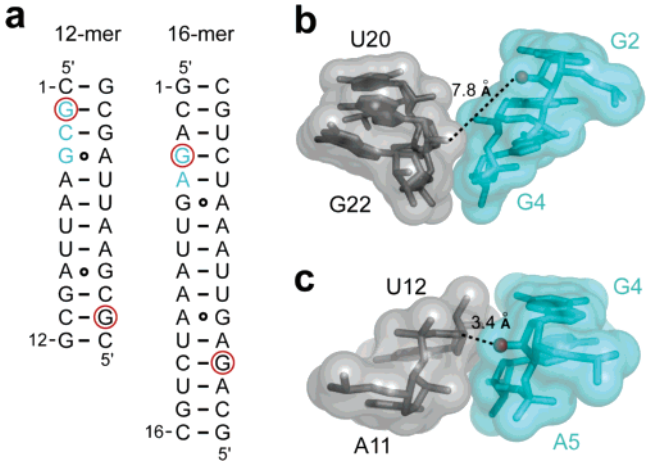

Figure 4. Location of the guanosine residues chosen for the 2′-methylseleno modifications (circled in red) in the structures of the nonmodified duplex RNAs, 12-mer[19] and 16-mer[20] (a). Crystal contact regions between two RNA molecules (gray and cyan sticks) are apparent in the surface representation of 12-mer (b) and 16-mer (c) RNAs. Nucleotides shown in cyan in (b) and (c) are indicated in RNAs (a). 2′-Oxygens for 2′-methylseleno modifications are shown as red spheres and the minimal distances to neighboring RNA molecules are indicated.

interfere with the formation of crystal contacts.[14] To investigate the impact of these modifications on RNA crystallization, we placed 2′-methylseleno guanosine residues into the 12 nt and 16 nt RNAs in positions (Figure 4a) which are located close to (12-mers, Figure 4b) or within (16-mers, Figure 4b) the regions of intermolecular crystal contacts.[19,20] Since these RNAs form double-stranded helices in the crystal lattice that are packed in a head-to-tail fashion with just a few side-to-side contacts, the effect of Se modification on crystallization should be maximized at least in the 16 nt RNA **13a**.

Interestingly, both Se-modified RNAs, **12a** and **13a**, were not crystallized in the conditions published for the nonmodified RNAs,[19,20] although control nonmodified RNAs readily produced diffracting crystals. To investigate the ability of the Se-modified RNAs to crystallize, we performed a search for crystallization conditions using commercial sparse matrix kits. Both 12 nt and 16 nt Se-modified RNAs along with their nonmodified counterparts were screened using 146 unique conditions at 4 and 20 °C. Remarkably, the Se-modified RNAs **12a** and **13a** produced crystals with a larger number of solutions than their nonmodified counterparts did (total 17 versus 15 for the 12-mers and 33 versus 24 for the 16-mers). However, this increase was predominantly due to the appearance of thin needle-shaped crystal plates growing from the common center ('RNA flowers')[25] for **12a** (7 conditions) and a higher number of microcrystals for **13a** (26 versus 11). A count of large-shaped crystals was clearly greater for the nonmodified RNAs (3 versus 1 for the 12-mers and 13 versus 7 for the 16-mers). Importantly, successful crystallization conditions for the nonmodified and Se-modified RNAs overlapped only partially (10 for the 12-mers and 19 conditions for the 16-mers, respectively). A large number of the Se-modified RNAs was crystallized in new unique conditions. This means that Se modification can be viewed as a new sequence variation of RNA targets to find diffraction-quality crystals. It is not clear, however, if this increase can be explained by the particular placement of selenium atoms or by the lower solubility of the 2′-methylseleno-modified RNAs. Nevertheless, such behavior of Se-modified RNAs can be paralleled with well-known properties of Se-Met-modified proteins, which sometimes do not produce crystals in the established conditions and require adjustment of crystallization conditions or even new crystallization screenings.

Crystal Structure of the 2′-Methylseleno-Modified 16 nt RNA. Among many solution conditions suitable for crystallization of the Se-modified RNAs, two, based on lithium sulfate and PEG4000, respectively, yielded large well-diffracting crystals of the 16 nt RNA **13a** (see Experimental Section). Remarkably, the nonmodified 16-mer produced only microcrystals in the same conditions. Both "lithium sulfate" and "PEG4000" crystals belonged to the *R*3 space group (Table 2), originally found in the crystals of the nonmodified RNA.[20] The crystals had similar cell unit parameters with *a*/*b* dimensions 6.0% and 8.9% longer than those in the original structure, clearly

(25) Hollbrook, S. R.; Hollbrook, E. I.; Walukiewicz, H. E. *Cell. Mol. Life Sci.* **2001**, *58*, 234−243.

Table 2. X-ray Data Collection and Refinement Statistics.[a,b]

	16-mer PEG4000			16-mer PEG4000	16-mer Li_2SO_4
Data Collection					
space group	*R*3			*R*3	*R*3
cell dimensions (hexagonal settings)					
a, *b*, *c* (Å)	45.06, 45.06, 128.20			45.47, 45.47, 128.91	46.31, 46.31, 128.35
α, β, γ (deg)	90, 90, 120			90, 90, 120	90, 90, 120
resolution[a]	20−3.0 (3.11−3.0)			20−2.9 (3.0−2.9)	20−2.9 (3.0−2.9)
	peak	inflection	remote		
wavelength (Å)	0.978901	0.979113	0.968634	0.979096	0.978948
R_{sym} (%)[a]	10.6 (34.4)	10.1 (36.3.9)	10.4 (34.8)	10.9 (31.6)	11.2 (32.0)
$\langle I \rangle / \sigma(I)$[a]	14.6 (6.0)	16.3 (4.0)	16.4 (6.7)	32.3 (10.1)	12.7 (6.5)
completeness (%)[a]	99.9 (100)	99.9 (100)	99.8 (100)	99.9 (100)	97.2 (99.5)
measured reflections	11079	11097	11061	23518	13676
unique reflections[a]	1970 (194)	1975 (193)	1970 (194)	2198 (220)	2227 (221)
Refinement					
resolution (Å)				20−2.9 (2.97−2.9)	20−2.9 (2.97−2.9)
number of reflections				2095	2118
working set				1966	2016
test set				99	102
completeness				99.68 (100.0)	97.2 (99.4)
R_{work}/R_{free} (%)[a]				23.0/25.5	21.2/23.9
number of atoms				680	695
RNA				680	680
mean B-factor (Å^2)				52.9	35.2
rmsd from ideality					
bond lengths (Å)				0.005	0.005
bond angles (deg)				1.103	1.125
estimated coordinate error (Å)[b]				0.47	0.32

[a] Values for the highest resolution shell are in parentheses. [b] Estimated coordinate error based on maximum likelihood was calculated with REFMAC (ref 49).

suggesting possible alterations in the crystal packing. The X-ray structures determined from the lithium sulfate and PEG4000 crystals were virtually identical (rmsd 0.55 Å) and, therefore, only the 2.9 Å lithium sulfate structure is described below.

The Se-modified 16 nt RNA **13a** was crystallized as a right-handed A-form duplex with two nonadjacent G•A mispairs separated by four Watson−Crick base pairs as described for the nonmodified RNA structure.[20] Using all-atom superimposition, the two structures can be superimposed with a rather large rmsd of 1.377 Å due to an almost doubled (∼8°) end-to-end bending in the Se-modified RNA calculated by CURVES (Figure 5a).[26] Characteristic nucleobase interactions of the original duplex, in particular the G(syn)•A^+(anti) mispairs, can also be modeled in the Se-modified structure (Figure 5b). Nevertheless, original N6(A)−O6(G) and N1(A)−N7(G) hydrogen bond patterns are not preserved due to longer N1(A)−N7(G) distances (4.38 and 3.53 Å). Therefore, in the Se-modified RNA both G•A^+ mispairs are held by O6(G)−N1(A) hydrogen bonds (2.52 and 2.71 Å) with the potential formation of an O6(G6)−N6(A27) hydrogen bond (2.78 Å). It is worth mentioning that the electron density map for the G•A mispairs (Figure 5b) is slightly worse than the base pairs closer to the RNA tips, suggesting some "breathing" within the structure. Such "breathing" is supported by higher *B*-factor values in the middle part of the duplex and it may even cause alternate G•A pairing in different molecules of the crystal. The formation of different G•A base pairs at the same sequence position is not that surprising since the conformation of these mismatches is sensitive to various factors.[27−32]

Intermolecular Contacts in the Crystal Lattice. Our analysis of the crystal contacts revealed that the RNA helices of **13a** are packed in the head-to-tail fashion, making a few side-to-side interactions with two neighboring RNA helices. In contrast to the nonmodified RNAs (Figure 5c), the central region of the Se-modified RNAs is not involved in packing interactions (Figure 5d). In addition, two stacked helices (green and gray, Figure 5c) of the nonmodified RNA make side-to-side contacts with the same neighboring helix (blue), while the Se-modified helices do not form such overlapping interactions (Figure 5d, Supporting Information Tables S1 and S2). Another rather noticeable difference between the two types of packing is the orientation of G4 and G20 (red nucleotides on Figure 5c,d). In the nonmodified RNA, these nucleotides face the opposite strand of the neighboring helix, but in the presence of Se modifications (Figure 5e) they are positioned against the same nucleotides. Moreover, three Se atoms from neighboring molecules are located at a close (∼4.0 Å) distance from each other (Figure 5f). The atoms form an equilateral triangle in the center of the packing interactions, thus placing nine nucleotides from three RNA molecules into close proximity, and therefore directly and significantly contributing toward bringing these RNA helices together. Since these packing interactions are exclusive for the Se-modified RNAs and are characteristic of the crystals grown in rather different conditions with either salt or organic polymer as precipitating agents, we suggest that the 2′-methylseleno modification is an important driving force in the packing of RNA helices.

Conclusion

With the synthesis of the guanosine phosphoramidite **10** and its facile incorporation into RNA by solid-phase synthesis, we

(26) Lavery, R.; Sclenar, H. *J. Biomol. Struct. Dyn*. **1989**, *4*, 655−667.
(27) SantaLucia, J.; Turner, D. H. *Biochemistry* **1993**, *32*, 12612−12623.
(28) Wu, M.; Turner, D. H. *Biochemistry* **1996**, *35*, 9677−9689.
(29) Wu, M.; SantaLucia, J.; Turner, D. H. *Biochemistry* **1997**, *36*, 4449−4460.
(30) Heus, A. H.; Wijmenga, S. S.; Hoppe, H.; Hilbers, C. W. *J. Mol. Biol*. **1997**, *271*, 147−158.
(31) Gao, X.; Patel, D. J. *J. Am. Chem. Soc*. **1988**, *110*, 5178−5182.
(32) Carbonnaux, C.; van der Marel, G. A.; van Boom, J. H.; Guschlbauer, W.; Fazakerley, G. V. *Biochemistry* **1991**, *30*, 5449−5458.

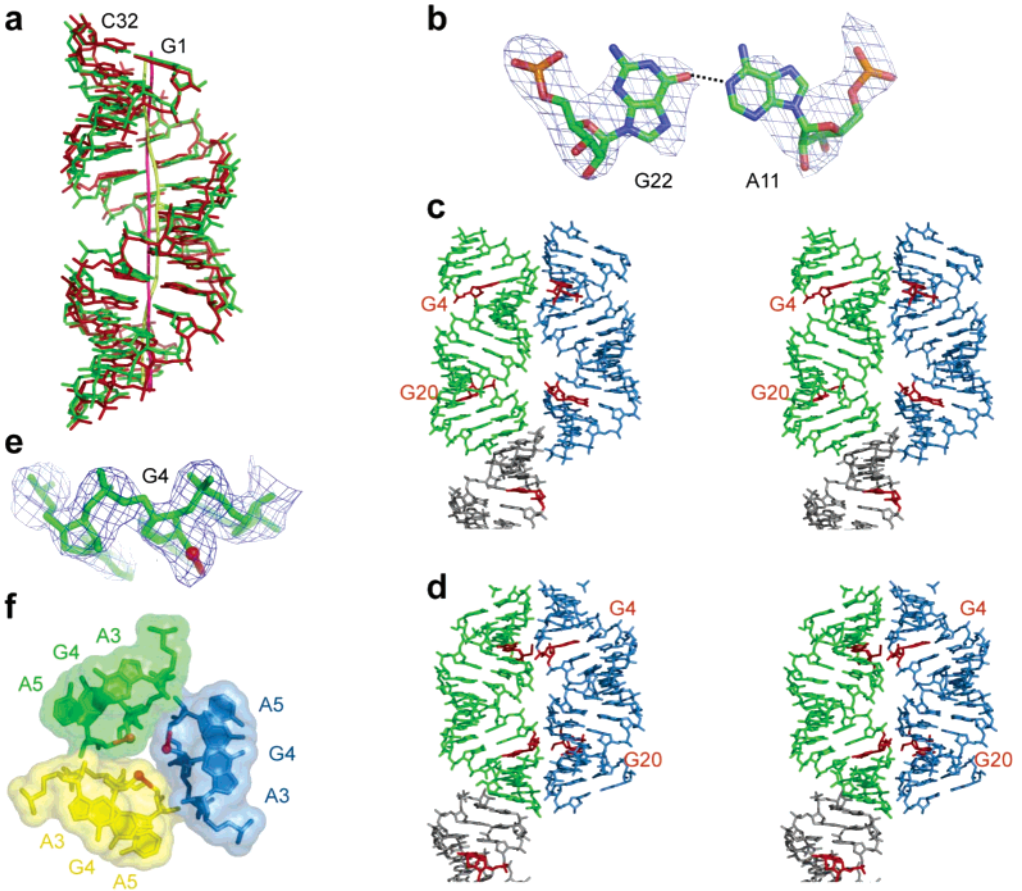

Figure 5. Crystal structure of the 2′-methylseleno-modified RNA duplex (rGCAG$_{Se}$AGUUAAAUCUGC)$_2$ (sequence **13a**) and comparison with its nonmodified counterpart. (a) Superimposition of the 2′-methylseleno-modified (green) and nonmodified (red) RNA structures and their curved helical axes (pink and light green, respectively). (b) G(syn)•A$^+$(anti) mispair shown with omit $F_o - F_c$ electron density map, contoured at 2σ level. Hydrogen bond is shown by dashed line. (c) Crystal packing of the nonmodified 16-mer RNA[20] in stereo representation. Side-to-side packing contacts are shown for three neighboring helices (green, blue, and gray) depicted in stick representations. Guanosines chosen for the Se modifications are in red. (d) Crystal packing of the 2′-methylseleno-modified 16-mer RNA presented in the same way as Figure 5c. Guanosines with the 2′-methylseleno modifications are in red. (e) Omit $2F_o - F_c$ electron density map for the region around 2′-methylseleno-modified residue G4, calculated without G4 and contoured at 1σ level. Red sphere and stick show Se atom and methyl group. (f) Packing contacts between three Se-modified RNAs (green, yellow, and blue sticks and surfaces) involving 2′-methylseleno groups (red spheres for Se atoms and sticks for methyl groups).

have complemented the set of previously reported 2′-methylseleno-modified uridine, cytidine, and adenosine building bocks and continue to establish Se-modified RNA as a powerful tool in RNA X-ray structure analysis. Moreover, our detailed investigations on the redox behavior of 2′-methylseleno-guanosine-containing RNA shed light on the requirement to expose Se-RNA to DTT during synthesis, deprotection, and crystallization since the presence of DTT reduces selenoxides and therefore guarantees a uniformly labeled RNA.

For X-ray structure analysis, we consider RNA with covalent 2′-methylseleno groups best applicable for sizes up to about 80 nucleotides. Se-RNA of this dimension can be readily obtained by solid-phase synthesis in combination with enzymatic ligation procedures as shown previously.[4] For RNAs up to about 35 nt, the Se approach is in competition with 5-iodo and 5-bromo pyrimidine derivatization.[33−39] We render the Se approach superior since all four 2′-methylseleno nucleoside phosphoramidites are now available, and therefore a great flexibility for adequate positioning within the RNA target is attained. In addition, 5-halogen pyrimidine derivatives are highly photoreactive species.[40−42] Inherent radiation damage of 5-halogen-modified nucleic acids during MAD data collection has been reported as a limitation.[37] For medium-size RNA (up to 100 nt), the Se approach competes with heavy metal ion derivatization.[43−46] Heavy atom search is a time-consuming process which requires soaking of the RNA crystals with dozens of compounds at various concentrations, therefore demanding many reasonably good crystals. This can be a serious obstacle, as had been encountered for the Diels−Alder ribozyme where the Se

(33) Shui, X.; Peek, M. E.; Lipscomb, L. A.; Gao, Q.; Ogata, C.; Roques, B. P.; Garbay-Jaureguiberry, C.; Wilkinson, A. P.; Williams, L. D. *Curr. Med. Chem.* **2000**, *7*, 59−71.
(34) Deng, J.; Xiong, Y.; Sundaralingam M. *Proc. Natl. Acad. Sci. U.S.A.* **2001**, *98*, 13665−13670.
(35) Wing, R.; Drew, H.; Takano, T.; Broka, C.; Tanaka, S.; Itakura, K.; Dickerson, R. E. *Nature* **1980**, *287*, 755−758.
(36) Zhang, L.; Doudna, J. A. *Science* **2002**, *295*, 2084−2088.
(37) Ennifar, E.; Carpentier, P.; Ferrer, J. L.; Walter, P.; Dumas, P. *Acta Crystallogr., D* **2002**, *58*, 1262−1268.
(38) Nowakowski, J.; Shim, P. J.; Stout, D.; Joyce, G. F. *J. Mol. Biol.* **2000**, *300*, 93−102.
(39) Correll, C. C.; Freeborn, B.; Moore, P. B.; Steitz, T. A. *Cell* **1997**, *91*, 705−712.
(40) Gott, J. M.; Wu, H.; Koch, T. H.; Uhlenbeck, O. C. *Biochemistry* **1991**, *30*, 6290−6295.
(41) Xu, Y.; Sugiyama, H. *J. Am. Chem. Soc.* **2004**, *126*, 6274−6279.
(42) Zeng, Y.; Wang, Y. *J. Am. Chem. Soc.* **2004**, *126*, 6552−6553.
(43) Golden, B. L. *Methods Enzymol.* **2000**, *317*, 124−132.
(44) Ennifar, E.; Walter, P.; Dumas, P. *Acta Crystallogr.* **2001**, *D57*, 330−332.
(45) Francois, B.; Lescoute-Phillips, A.; Werner, A.; Masquida, B. In *Handbook of RNA Biochemistry Volume 1*; Hartmann, R. K., Bindereif, A., Schön, A., Westhof, E., Eds.; Wiley-VCH: New York, 2005; pp 438−452.
(46) Ke, A.; Doudna, J. A. *Methods* **2004**, *34*, 408−414.

approach finally delivered the key derivative to enable structure determination.[12] Despite the similarity between the native and Se-modified Diels−Alder ribozymes, we anticipated that 2′-methylseleno groups may interfere with RNA crystallization if placed in the regions of the crystal packing interactions. Our crystallization experiments clearly indicate that even in the worst case, when modifications are located in the regions of intermolecular contacts and perturb established crystallization protocols, additional screening may identify many more crystallization conditions. These conditions, however, can produce crystals with the same space group but different crystal packing interactions, necessitating the careful analysis of the crystal isomorphism prior usage of native and selenium data in phase calculations. Nevertheless, the X-ray structures presented here demonstrate that even in the presence of a novel set of packing interactions, possibly driven by 2′-methylseleno modifications, overall RNA conformation and even fine structural details are largely preserved. Our crystallization experiments, therefore, suggest a novel role for 2′-methylseleno modifications, namely, expanding the search for new crystal forms and potentially even forcing crystallization of former noncrystallizable RNA molecules.

Experimental Section

Synthesis of 2′-Methylseleno Guanosine Phosphoramidite (10). General. ^{1}H, ^{13}C, and ^{31}P NMR spectra were recorded on a Bruker DRX 300 MHz, or Varian Unity 500 MHz instrument. The chemical shifts are reported relative to TMS and referenced to the residual proton signal of the deuterated solvents: $CDCl_3$ (7.26 ppm), d_6-DMSO (2.50 ppm) for ^{1}H NMR spectra; $CDCl_3$ (77.0 ppm) or d_6-DMSO (39.5 ppm) for ^{13}C NMR spectra. ^{31}P shifts are relative to external 85% phosphoric acid. ^{1}H- and ^{13}C-assignments were based on COSY and HSQC experiments. UV-spectra were recorded on a Varian Cary 100 spectrophotometer. Analytical thin-layer chromatography (TLC) was carried out on silica 60F-254 plates. Flash column chromatography was carried out on silica gel 60 (230−400 mesh). Packing of silica gel columns was performed with 1% Et_3N added to the corresponding starting eluent. All reactions were carried out under an Ar atmosphere. 9-[β-D-Arabinofuranosyl]guanine **1** was obtained from *MetkinenOy*, Finland. Chemical reagents and solvents were purchased from commercial suppliers and used without further purification. Organic solvents for reactions were dried overnight over freshly activated molecular sieves (4 Å).

9-[3′,5′-*O*-(1,1,3,3-Tetraisopropyldisiloxane-1,3-diyl)-β-D-arabinofuranosyl]guanine (2). 9-[β-D-Arabinofuranosyl]guanine **1** (4.16 g; 14.7 mmol) was coevaporated with dry pyridine three times and then suspended in DMF (160 mL) and pyridine (14 mL) under an argon atmosphere. After dropwise addition of 1,3-dichloro-1,1,3,3-tetraisopropyldisiloxane (4.86 g, 15.4 mmol), the reaction mixture was stirred at room temperature for 16 h and subsequently precipitated by being poured into ice−water that was vigorously stirred (2.6 L). The crude product was collected on a glass-fritted Büchner funnel and used without further purification for the next step. For analysis, a small portion of crude product was crystallized from ethanol. Yield: 7.60 g of **2** as white powder (98%). TLC (CH_2Cl_2/MeOH, 85/15): $R_f = 0.65$. ^{1}H NMR (300 MHz, d_6-DMSO): δ 1.06 (m, 28H, $(i\text{Pr})_4Si_2O$); 3.74 (m, 1H, H−C(4′)); 3.95 (m, 2H, H1−C(5′) and H2−C(5′)); 4.30 (m, 1H, H−C(3′)); 4.42 (m, 1H, H−C(2′)); 5.78 (d, $J = 5.9$ Hz, 1H, HO−C(2′)); 5.95 (d, $J = 6.4$ Hz, 1H, H−C(1′)); 6.43 (s, 2H, NH_2); 7.60 (s, 1H, H−C(8)); 10.57 (s, 1H, H−N(1)) ppm. ^{13}C NMR (75 MHz, d_6-DMSO): δ 11.93, 12.26, 12.40, 12.77, 16.73, 16.81, 16.88, 17.09, 17.11, 17.13, 17.26 (iPr)$_4Si_2O$); 61.23 (C(5′)); 74.48 (C(2′)); 75.34 (C(3′)); 79.44 (C(4′)); 80.49 (C(1′)); 115.79 (C(ar)); 135.86 (C(8)); 151.25, 153.64, 156.67 (C(ar)) ppm. UV (MeOH): $\lambda_{max} = 252$ nm. ESI-MS (m/z): calcd for $C_{22}H_{39}N_5O_6Si_2$ $[M + H]^+$ 526.76, found 526.10, $[M + Na]^+$ 548.74, found 548.17.

***N*^{2}-Acetyl-9-[2′-*O*-acetyl-3′,5′-*O*-(1,1,3,3-tetraisopropyldisiloxane-1,3-diyl)-β-D-arabinofuranosyl]guanine (3a) and *N*^{2},*N*^{2}-Diacetyl-9-[2′-*O*-acetyl-3′,5′-*O*-(1,1,3,3-tetraisopropyldisiloxane-1,3-diyl)-β-D-arabinofuranosyl]guanine (3b).** Compound **2** (7.00 g, 13.3 mmol) was coevaporated with dry pyridine three times and then suspended in DMF (80 mL), pyridine (80 mL), and acetic anhydride (80 mL) under an argon atmosphere. The reaction mixture was stirred for 16 h at 80 °C. The solvents were removed under vacuum and the residual brown viscous oil was partitioned between dichloromethane (500 mL) and an aqueous solution containing 5% citric acid. The organic layer was separated and the aqueous layer was extracted four times with dichloromethane (700 mL). The combined organic layers were washed with saturated aqueous NaCl (600 mL), dried over Na_2SO_4, and concentrated under vacuum. The crude product was purified by column chromatography on SiO_2 (CH_2Cl_2/MeOH, 99/1−92/8 v/v). Yield: 2.91 g of **3a**; 5.20 g of **3a** + **3b** as colorless foam (64%). A mixture of **3a** and **3b** can be used in the next reaction step. TLC (CH_2Cl_2/MeOH, 9/1): $R_f = 0.57$ (**3b**), 0.63 (**3a**). Characterization data of **3a**: ^{1}H NMR (300 MHz, $CDCl_3$): δ 0.95−1.05 (m, 28H, $(i\text{Pr})_4Si_2O$); 1.75 (s, 3H, $COCH_3$); 2.30 (s, 3H, $NHCOCH_3$); 3.87 (m, 1H, H−C(4′)); 4.08 (m, 2H, H1−C(5′) and H2−C(5′)); 4.64 (m, 1H, H−C(3′)); 5.49 (m, 1H, H−C(2′)); 6.26 (d, $J = 6.4$ Hz, 1H, H−C(1′)); 7.97 (s, 1H, H−C(8)); 9.58 (s, 1H, H−N(1)); 12.03 (s, 1H, HN−C(2)) ppm. ^{13}C NMR (75 MHz, $CDCl_3$): δ 12.38, 12.85, 13.03, 13.35, 16.70, 16.72, 16.83, 16.89, 17.26, 17.34, 17.42 (iPr)$_4Si_2O$); 20.07 ($COCH_3$); 24.29 ($NHCOCH_3$); 60.60 (C(5′)); 71.14 (C(3′)); 76.40 (C(2′)); 80.36 (C(4′)); 80.44 (C(1′)); 120.81 (C(ar)); 137.61 (C(8)); 147.52, 148.14, 155.66 (C(ar)); 169.83, 172.11 (2 × $COCH_3$) ppm. UV (MeOH): $\lambda_{max} = 256$ nm. ESI-MS (m/z): calcd for $C_{26}H_{43}N_5O_8Si_2$ $[M + H]^+$ 610.82, found 610.10, $[M + Na]^+$ 632.81, found 632.26.

***N*^{2}-Acetyl-9-[2′-*O*-acetyl-3′,5′-*O*-(1,1,3,3-tetraisopropyldisiloxane-1,3-diyl)-β-D-arabinofuranosyl]-*O*^{6}-[2-(4-nitrophenyl)ethyl]guanine (4a) and *N*^{2},*N*^{2}-Diacetyl-9-[2′-*O*-acetyl-3′,5′-*O*-(1,1,3,3-tetraisopropyldisiloxane-1,3-diyl)-β-D-arabinofuranosyl]-*O*^{6}-[2-(4-nitrophenyl)ethyl]guanine (4b).** Compound **3a** (4.65 g, 7.48 mmol), triphenylphosphine (2.94 g, 11.2 mmol), and 2-(4-nitrophenyl)ethanol (1.88 g, 11.2 mmol) were coevaporated with dry dioxane and then suspended in dioxane (150 mL). After 30 min of stirring, diisopropyl azodicarboxylate (2.36 mL, 12.0 mmol) was added and stirring continued for 45 min. The solvents were removed under vacuum and the residue was partitioned between dichloromethane (500 mL) and saturated sodium bicarbonate solution. The organic layer was separated, and the aqueous layer was extracted twice with dichloromethane (700 mL). The combined organic layers were dried over Na_2SO_4 and evaporated. The crude product was purified by column chromatography on SiO_2 (hexanes/EtOAc, 9/1−5/5 v/v). Yield: 3.63 g of **4a** as yellowish foam (64%). Likewise, a mixture of **3a** and **3b** was used as starting material. Separation of **4a** and **4b** was performed by column chromatography on SiO_2 (hexanes/EtOAc, 9/1−5/5 v/v). TLC (hexanes/EtOAc, 2/8): $R_f = 0.55$ (**4a**), 0.72 (**4b**). Characterization data of **4a**: ^{1}H NMR (300 MHz, $CDCl_3$): δ 0.98−1.25 (m, 28H, $(i\text{Pr})_4Si_2O$); 1.71 (s, 3H, $COCH_3$); 2.56 (s, 3H, $NHCOCH_3$); 3.31 (t, $J = 6.8$ Hz, 2H, $CH_2-C_6H_4-NO_2$); 3.90 (m, 1H, H−C(4′)); 4.10 (m, 2H, H1−C(5′) and H2−C(5′)); 4.69 (m, 1H, H−C(3′)); 4.74 (m, 2H, O^6-CH_2); 5.56 (m, 1H, H−C(2′)); 6.41 (d, $J = 6.2$ Hz, 1H, H−C(1′)); 7.50 (d, $J = 8.5$ Hz, 2H, 4-nitrophenyl H−C(2)/H−C(6)); 7.84 (s, 1H, HN−C(2)); 8.09 (s, 1H, H−C(8)); 8.18 (d, $J = 8.5$ Hz, 2H, 4-nitrophenyl H−C(3)/H−C(5)) ppm. ^{13}C NMR (75 MHz, $CDCl_3$): δ 12.40, 12.97, 13.03, 13.39, 16.73, 16.83, 16.90, 17.26, 17.32, 17.39, 17.42 ((iPr)$_4Si_2O$); 20.02 ($COCH_3$); 25.13 ($NHCOCH_3$); 35.05 ($CH_2-C_6H_4-NO_2$); 60.55 (C(5′)); 66.90 (O^6-CH_2); 71.29 (C(3′)); 76.38 (C(2′)); 80.54 (C(4′)); 80.56 (C(1′)); 117.28 (C(ar)); 123.78 (4-nitrophenyl C(2)/C(6)); 129.92 (4-nitrophenyl C(3)/C(5)); 140.28 (C(8)); 145.48, 146.97, 152.23, 152.78, 160.55 (C(ar)); 169.35, 172.00 ($COCH_3$) ppm. UV (MeOH): $\lambda_{max} =$

269 nm. ESI-MS (*m*/*z*): calcd for $C_{34}H_{50}N_6O_{10}Si_2$ $[M + H]^+$ 759.97, found 759.26, $[M + Na]^+$ 781.96, found 781.42. Characterization data of **4b**: ^{1}H NMR (300 MHz, $CDCl_3$): δ 0.99−1.17 (m, 28H, $(iPr)_4Si_2O$); 1.69 (s, 3H, $COCH_3$); 2.27 (s, 6H, 2 × $COCH_3$); 3.30 (t, J = 6.9 Hz, 2H, $CH_2-C_6H_4-NO_2$); 3.91 (m, 1H, H−C(4′)); 4.10 (m, 2H, H1−C(5′) and H2−C(5′)); 4.78 (m, 1H, H−C(3′)); 4.79 (m, 2H, O^6-CH_2); 5.55 (dd, J = 6.4, 8.0 Hz, 1H, H−C(2′)); 6.44 (d, J = 6.4 Hz, 1H, H−C(1′)); 7.46 (d, J = 8.7 Hz, 2H, 4-nitrophenyl H−C(2)/H−C(6)); 7.84 (s, 1H, HN−C(2)); 8.15 (d, J = 8.7 Hz, 2H, 2H, 4-nitrophenyl H−C(3)/H−C(5)); 8.26 (s, 1H, H−C(8)) ppm. ^{13}C NMR (75 MHz, $CDCl_3$): δ 12.38, 12.97, 12.99, 13.33, 16.72, 16.84, 16.89, 17.26, 17.33, 17.38, 17.42 ($(iPr)_4Si_2O$); 19.88 ($COCH_3$); 26.01 (2 × $COCH_3$); 35.02 ($CH_2-C_6H_4-NO_2$); 61.08 (C(5′)); 67.33 (O^6-CH_2); 72.04 (C(3′)); 76.72 (C(2′)); 80.76 (C(4′)); 81.28 (C(1′)); 120.42 (C(ar)); 123.77 (4-nitrophenyl C(2)/C(6)); 129.92 (4-nitrophenyl C(3)/C(5)); 142.75 (C(8)); 145.27, 147.00, 152.53, 152.87, 161.26 (C(ar)); 169.43, 171.87 ($COCH_3$) ppm. UV (MeOH): λ_{max} = 260 nm. ESI-MS (*m*/*z*): calcd for $C_{36}H_{52}N_6O_{11}Si_2$ $[M + H]^+$ 802.00, found 801.07, $[M + Na]^+$ 823.99, found 823.31.

***N*²-Acetyl-9-[3′,5′-*O*-(1,1,3,3-tetraisopropyldisiloxane-1,3-diyl)-β-D-arabinofuranosyl]-*O*⁶-[2-(4-nitrophenyl)ethyl]guanine (5).** Compound **4a** (3.41 g, 4.49 mmol) was dissolved in THF/MeOH (5/4; 130 mL) and stirred at 0 °C, and NaOH (0.5 M, 150 mL) was added. After 7 min acetic acid (0.5 M, 160 mL) was added. The solvents were evaporated and the residue was dissolved in dichloromethane (400 mL), washed with water (400 mL), dried over Na_2SO_4, and evaporated. The crude product was purified by column chromatography on SiO_2 (CH_2Cl_2/MeOH, 99/1−98/2 v/v). Yield: 1.84 g of 5 colorless foam (57%). Likewise, a mixture of **4a** and **4b** was used as starting material. TLC (hexanes/EtOAc, 2/8): R_f = 0.46. ^{1}H NMR (300 MHz, $CDCl_3$): δ 1.01−1.14 (m, 28H, $(iPr)_4Si_2O$); 2.37 (s, 3H, $COCH_3$); 2.29 (t, J = 6.8 Hz, 2H, $CH_2-C_6H_4-NO_2$); 3.86 (m, 1H, H−C(4′)); 4.05 (m, 2H, H1−C(5′) and H2−C(5′)); 4.51 (t, J = 7.3 Hz, 1H, H−C(3′)); 4.30 (s, 1H, HO−C(2′)); 4.64 (m, 1H, H−C(2′)); 4.74 (m, 2H, O^6-CH_2); 6.14 (d, J = 5.7 Hz, 1H, H−C(1′)); 7.49 (d, J = 8.7 Hz, 2H, 4-nitrophenyl H−C(2)/H−C(6)); 8.07 (s, 1H, HN−C(2)); 8.14 (s, 1H, H−C(8)); 8.16 (d, J = 8.7 Hz, 2H, 4-nitrophenyl H−C(3)/H−C(5)) ppm. ^{13}C NMR (75 MHz, $CDCl_3$): δ 12.46, 13.00, 13.08, 13.50, 16.89, 16.95, 17.05, 17.32, 17.39, 17.48 ($(iPr)_4Si_2O$); 24.95 ($COCH_3$); 35.02 ($CH_2-C_6H_4-NO_2$); 61.49 (C(5′)); 67.01 (O^6-CH_2); 74.59 (C(3′)); 76.75 (C(2′)); 81.75 (C(4′)); 83.82 (C(1′)); 117.67 (C(ar)); 123.79 (4-nitrophenyl C(2)/C(6)); 129.91 (4-nitrophenyl C(3)/C(5)); 141.43 (C(8)); 145.44, 146.96, 151.56, 152.47, 160.21 (C(ar)), 169.87 ($COCH_3$) ppm. UV (MeOH): λ_{max} = 260 nm. ESI-MS (*m*/*z*): calcd for $C_{32}H_{48}N_6O_9Si_2$ $[M + H]^+$ 717.93, found 717.11, $[M + Na]^+$ 739.92, found 739.29.

***N*²-Acetyl-9-{2′-*O*-[(trifluoromethyl)sulfonyl]-3′,5′-*O*-(1,1,3,3-tetraisopropyldisiloxane-1,3-diyl)-β-D-arabinofuranosyl}-*O*⁶-[2-(4-nitrophenyl)ethyl]guanine (6).** Compound **5** (600 mg, 0.837 mmol) was coevaporated with dry pyridine and dissolved in CH_2Cl_2 (100 mL). DMAP (153 mg, 1.26 mmol) and triethylamine (169 mg, 233 μL, 1.67 mmol) were added and the reaction mixture was cooled to 0 °C. Then, trifluoromethanesulfonyl chloride (211 mg, 158 μL, 1.26 mmol) was added and the mixture was stirred for 2 h. The reaction mixture was diluted with dichloromethane, washed with saturated sodium bicarbonate solution, dried over Na_2SO_4, and evaporated. The crude product was purified by column chromatography on SiO_2 (hexanes/EtOAc, 9/1−5/5 v/v). Yield: 490 mg of **6** as colorless foam (69%). TLC (hexanes/EtOAc, 50/50): R_f = 0.44. ^{1}H NMR (300 MHz, $CDCl_3$): 1.00−1.16 (m, 28H, $(iPr)_4Si_2O$); 2.55 (s, 3H, $COCH_3$); 3.35 (t, J = 6.8 Hz, 2H, $CH_2-C_6H_4-NO_2$); 3.94 (m, 1H, H−C(4′)); 4.12 (m, 2H, H1−C(5′) and H2−C(5′)); 4.83 (t, J = 6.8 Hz, 2H, O^6-CH_2); 4.95 (m, 1H, H−C(3′)); 4.30 (s, 1H, HO−C(2′)); 5.46 (m, 1H, H−C(2′)); 6.42 (d, J = 5.9 Hz, 1H, H−C(1′)); 7.49 (d, J = 8.7 Hz, 2H, 4-nitrophenyl H−C(2)/H−C(6)); 7.88 (s, 1H, HN−C(2)); 8.05 (s, 1H, H−C(8)); 8.17 (d, J = 8.7 Hz, 2H, 4-nitrophenyl H−C(3)/H−C(5)) ppm. ^{13}C NMR (75 MHz, $CDCl_3$): δ 12.64, 12.97, 13.10, 13.23, 16.59, 16.72, 16.80, 17.20, 17.30, 17.37 ($(iPr)_4Si_2O$); 25.06 ($COCH_3$); 35.03 ($CH_2-C_6H_4-NO_2$); 61.00 (C(5′)); 67.02 (O^6-CH_2); 72.67 (C(3′)); 80.00 (C(1′)); 80.86 (C(4′)); 87.72 (C(2′)); 117.45 (C(ar)); 123.80 (4-nitrophenyl C(2)/C(6)); 129.90 (4-nitrophenyl C(3)/C(5)); 139.71 (C(8)); 145.40, 147.00, 152.31, 152.77, 160.70 (C(ar)); 170.59 ($COCH_3$) ppm. UV (MeOH): λ_{max} = 268 nm. ESI-MS (*m*/*z*): calcd for $C_{33}H_{47}F_3N_6O_{11}SSi_2$ $[M + H]^+$ 849.99, found 849.37, $[M + Na]^+$ 871.98, found 871.27.

***N*²-Acetyl-3′,5′-*O*-(1,1,3,3-tetraisopropyldisiloxane-1,3-diyl)-*O*⁶-[2-(4-nitrophenyl)ethyl]-2′-deoxy-2′-methylselenoguanosine (7).** Sodium borohydride (64 mg, 1.70 mmol) was placed in a sealed 25 mL two necked round-bottom flask, dried on high vacuum for 15 min to deplete oxygen, kept under argon, and suspended in dry THF (2.3 mL). Dimethyl diselenide (55 μL, 0.57 mmol) was slowly injected into this suspension, followed by the dropwise addition of anhydrous ethanol; 0.4 mL was required until gas bubbles started to appear in the yellow mixture. The solution was stirred at room temperature for 1 h and the almost colorless solution was injected into a solution of **6** (230 mg, 0.27 mmol) in dry THF (2.7 mL). The reaction mixture was stirred at room temperature for 20 min. Then, aqueous 0.2 M triethylammonium acetate buffer (5 mL, pH 7) was added and the solution was reduced to half of its volume by evaporation. Dichloromethane was added and the organic layer was washed twice with 0.2 M triethylammonium acetate buffer and, finally, with saturated sodium chloride solution. The organic layer was dried over Na_2SO_4 and the solvent was evaporated. The crude product was purified by column chromatography on SiO_2 (hexanes/EtOAc, 85/15−4/6 v/v). Yield: 186 mg of **7** as colorless foam (87%). TLC (hexanes/EtOAc, 4/6): R_f = 0.49. ^{1}H NMR (300 MHz, $CDCl_3$): δ 0.97−1.10 (m, 28H, $(iPr)_4Si_2O$); 1.93 (s, 3H $SeCH_3$); 2.55 (s, 3H, $COCH_3$); 3.31 (t, J = 6.8 Hz, 2H, $CH_2-C_6H_4-NO_2$); 3.94 (dd, J = 4.4, 4.5 Hz, 1H, H−C(2′)); 4.06 (m, 2H, H1−C(5′) and H2−C(5′)); 4.16 (m, 1H, H−C(4′)); 4.75 (s, 1H, H−C(3′)); 4.78 (m, 2H, O^6-CH_2); 6.21 (d, J = 4.5 Hz, 1H, H−C(1′)); 7.49 (d, J = 8.7 Hz, 2H, 4-nitrophenyl H−C(2)/H−C(6)); 7.87 (s, 1H, HN−C(2)); 8.07 (s, 1H, H−C(8)); 8.16 (d, J = 8.7 Hz, 2H, 4-nitrophenyl H−C(3)/H−C(5)) ppm. ^{13}C NMR (75 MHz, $CDCl_3$): δ 12.68, 13.03, 13.14, 13.51, 16.85, 16.96, 16.97, 17.11, 17.27, 17.28, 17.35, 17.45 ($(iPr)_4Si_2O$); 25.13 ($COCH_3$); 35.03 ($CH_2-C_6H_4-NO_2$); 47.05 (C(2′)); 61.85 (C(5′)); 66.91 (O^6-CH_2); 71.69 (C(3′)); 84.65 (C(4′)); 89.68 (C(1′)); 118.34 (C(ar)); 123.76 (4-nitrophenyl C(2)/C(6)); 129.93 (4-nitrophenyl C(3)/C(5)); 139.87 (C(8)); 145.46, 146.97, 152.03, 152.31, 160.60 (C(ar)); 170.57 ($COCH_3$) ppm. UV (MeOH): λ_{max} = 269 nm. ESI-MS (*m*/*z*): calcd for $C_{33}H_{50}N_6O_8SeSi_2$ $[M + H]^+$ 794.92, found 794.97, $[M + Na]^+$ 816.93, found 817.15.

***N*²-Acetyl-2′-deoxy-2′-methylselenoguanosine (8).** Compound **7** (735 mg, 0.726 mmol) was dissolved in THF (25 mL) and treated with 1 M TBAF in THF (6 mL). The solution was stirred at room temperature for 2.5 h. The solvent was evaporated and the product was isolated by column chromatography on SiO_2 (CH_2Cl_2/MeOH, 97/3−93/7 v/v). Yield: 230 mg of **8** as colorless foam (79%). TLC (CH_2Cl_2/MeOH, 85/15): R_f = 0.45. ^{1}H NMR (300 MHz, d_6-DMSO): δ 1.63 (s, 3H $SeCH_3$); 2.18 (s, 3H, $COCH_3$); 3.57 (m, 2H, H1−C(5′) and H2−C(5′)); 3.97 (m, 1H, H−C(4′)); 4.01 (m, 1H, H−C(2′)); 4.31 (s, 1H, H−C(3′)); 5.02 (t, J = 5.5 Hz, 1H, HO−C(5′)); 5.82 (d, J = 4.6 Hz, 1H, HO−C(3′)); 6.14 (d, J = 9.1 Hz, 1H, H−C(1′)); 8.30 (s, 1H, H−C(8)); 11.68 (s, 1H, HN−C(2)); 12.05(s, 1H, H−N(1)) ppm. ^{13}C NMR (75 MHz, d_6-DMSO): δ 2.90 ($SeCH_3$); 24.21 ($COCH_3$); 46.82 (C2′); 62.05 (C(5′)); 73.23 (C(3′)); 87.71 (C(4′)); 88.89 (C(1′)); 120.46 (C(ar)); 138.24 (C(8)); 148.53, 149.31, 155.19, (C(ar)); 173.91 ($COCH_3$) ppm. UV (MeOH): λ_{max} = 277 nm. ESI-MS (*m*/*z*): calcd for $C_{13}H_{17}N_5O_5Se$ $[M + H]^+$ 403.26, found 403.76, $[M + Na]^+$ 425.25, found 426.04.

***N*²-Acetyl-5′-*O*-(4,4′-dimethoxytrityl)-2′-deoxy-2′-methylselenoguanosine (9).** Compound **8** (178 mg, 0.443 mmol) was coevaporated with dry pyridine and then dissolved in pyridine (2 mL). The solution was treated with 4,4′-dimethoxytrityl chloride (165 mg, 0.487 mmol) in two portions over a period of 1 h. Stirring was continued overnight. The

solvents were removed under vacuum and the residue was dissolved in dichloromethane, washed with 5% citric acid, water, and saturated sodium bicarbonate solution, dried over Na_2SO_4, and evaporated. The crude product was purified by column chromatography on SiO_2 (CH_2Cl_2/MeOH, 98/2−95/5 v/v). Yield: 184 mg of **9** as colorless foam (59%). TLC (CH_2Cl_2/MeOH, 9/1): $R_f = 0.56$. ^{1}H NMR (300 MHz, $CDCl_3$): δ 1.76 (s, 3H $SeCH_3$); 1.87 (s, 3H, $COCH_3$); 3.27 (m, 1H, H1−C(5′)); 3.45 (m, 1H, H2−C(5′)); 3.73, 3.74 (2s, 6H, OCH_3); 3.90 (m, 1H, HO−C(3′)); 4.11 (m, 1H, H−C(2′)); 4.29 (m, 1H, H−C(4′)); 4.57 (s, 1H, H−C(3′)); 5.98 (d, $J = 9.0$ Hz, 1H, H−C(1′)); 7.18−7.47 (m, 13H, trityl-H); 7.87 (s, 1H, H−C(8)); 9.63 (s, 1H, HN−C(2)); 12.11(s, 1H, H−N(1)) ppm. ^{13}C NMR (75 MHz, $CDCl_3$): δ 4.05 ($SeCH_3$); 23.78 ($COCH_3$); 49.03 (C(2′)); 55.25 (2 × OCH_3); 64.10 (C(5′)); 72.94 (C(3′)); 85.45 (C(4′)); 96.48 (C(ar)); 88.88 (C(1′)); 113.24, 121.47, 127.12, 127.95, 128.05, 130.03, 135.54, 135.80 (C(ar)); 138.36 (C(8)); 144.83, 147.53, 148.85, 155.82, 158.73 (C(ar)); 172.49 ($COCH_3$) ppm. UV (MeOH): $\lambda_{max} = 260$ nm. FT-ICR-ESI-MS (*m*/*z*): calcd for $C_{34}H_{35}N_5O_7Se$ $[M + H]^+$ 706.17833, found 706.17730.

***N*²-Acetyl-5′-*O*-(4,4′-dimethoxytrityl)-2′-deoxy-2′-methylselenoguanosine 3′-(2-cyanoethyl diisopropylphosphoramidite) (10).** Compound **9** (220 mg, 0.312 mmol) was dissolved in a mixture of ethyldimethylamine (228 mg, 337 μL, 2.24 mmol) in dry dichloromethane (2.5 mL) under argon. After 15 min at room temperature, 2-cyanoethyl *N*,*N*-diisopropylchlorophosphoramidite (111 mg, 0.468 mmol) was slowly added and the solution was stirred at room temperature for 2 h. The crude product was purified by column chromatography on SiO_2 (CH_2Cl_2/MeOH, 99.5/0.5−98.5/1.5 v/v). Yield: 248 mg of **10** as colorless foam (88%). TLC (CH_2Cl_2/MeOH, 97/3): $R_f = 0.63$. ^{1}H NMR (500 MHz, $CDCl_3$): δ 1.00−1.27 (m, 24H, 2 × $((CH_3)_2CH)_2N$); 1.37, 1.48 (s, 6H, 2x $SeCH_3$); 1.69, 1.73 (s, 6H, $COCH_3$); 2.24, 2.28 (2 × m, 2H, CH_2CN); 2.62, 2.66 (2 × t, 2H, CH_2CN); 3.15 (m, 2H, H1−C(5′)); 3.54−3.63 (m, 4H, $((CH_3)_2CH)_2N$, 2H, H2−C(5′), 2H, $POCH_2$); 3.77, 3.78 (2s, 12H, OCH_3); 3.91−3.99, 4.10−4.22 (2m, 2H, $POCH_2$); 4.36, 4.41 (m, 2H, H−C(4′)); 4.45 (m, 2H, H−C(2′)); 4.71, 4.76 (m, 1H, H−C(3′)); 6.01, 6.06 (2 × d, $J = 9.0$ Hz, 9.34 Hz, 2H, H−C(1′)); 6.80, 7.26, 7.40, 7.55 (4 × m, 26H, trityl-H); 7.80 (s, 2H, H−C(8)); 7.67 (s, 2H, HN−C(2)); 11.93 (s, 2H, H−N(1)) ppm. ^{31}P NMR (121 MHz, $CDCl_3$): δ 151.3, 150.4 ppm; UV (MeOH): $\lambda_{max} = 235$ nm. FT-ICR-ESI-MS (*m*/*z*): calcd for $C_{34}H_{35}N_5O_7Se$ $[M + H]^+$ 906.28639, found 906.28685.

Solid-Phase Synthesis of 2′-Methylseleno Nucleoside Containing RNAs. 2′-*O*-TOM standard nucleoside phosphoramidites and the corresponding CPG supports (1000 Å) were obtained from *GlenResearch*. All oligoribonucleotides containing 2′-methylseleno nucleosides were synthesized on *Pharmacia* instrumentation (Gene Assembler Plus or Special) following modified DNA/RNA standard methods containing an additional cycle step of treatment with DTT; detritylation (2.0 min): dichloroacetic acid/1,2-dichloroethane (4/96); coupling (3.0 min): phosphoramidites/acetonitrile (0.1 M × 120 μL) were activated by benzylthiotetrazole/acetonitrile (0.35 M × 360 μL); capping (3 × 0.4 min): (A) Ac_2O/sym-collidine/acetonitrile (20/30/50), (B) 4-(dimethylamino)pyridine/acetonitrile (0.5 M), A/B = 1/1; oxidation (1.0 min): I_2 (10 mM) in acetonitrile/sym-collidine/H_2O (10/1/5); DTT treatment (2.0 min): DTT (100 mM) in ethanol/ H_2O (2/3). A ready-to-use synthesis method file is documented in ref 4. Solutions of standard amidites, tetrazole solutions, and acetonitrile were dried over activated molecular sieves overnight. Solutions of 2′-methylseleno guanosine phosphoramidites were only dried for 4−6 h over activated molecular sieves before consumption.

Deprotection and Purification of 2′-Methylseleno Nucleoside Containing RNAs. Prior to deprotection and cleavage from the solid support the Se-containing RNAs were treated with DTT in ethanol/ H_2O 1/1 (150 mM, 200 μL) for 1−3 h at room temperature. Then, $MeNH_2$ in EtOH (8 M, 0.60 mL), $MeNH_2$ in H_2O (40%, 0.60 mL), and DTT in EtOH/H_2O 1/1 (2 M, 95 μL; final DTT concentration 150 mM) were added and deprotection was continued for 5−6 h. After the solution was completely evaporated, tetrabutylammonium fluoride trihydrate (TBAF·3H_2O) in THF (1 M, 0.95 mL) was added. The reaction mixture was slowly shaken for at least 12 h at room temperature to remove the 2′-*O*-silyl ethers. The reaction was quenched by the addition of triethylammonium acetate (TEA) (1 M, pH 7.4, 0.95 mL). The volume of the solution was reduced to 1 mL and the solution was loaded on a Amersham HiPrep 26/10 Desalting (2.6 × 10 cm; Sephadex G25). The crude RNA was eluted with H_2O and dried.

Analysis of crude RNA products after deprotection was performed by anion-exchange chromatography on a Dionex DNAPac100 column (4 × 250 mm) at 80 °C. Flow rate: 1 mL/min; eluant A: 25 mM Tris-HCl (pH 8.0), 6 M urea; eluant B: 25 mM Tris-HCl (pH 8.0), 0.5 M $NaClO_4$, 6 M urea; gradient: 0−60% B in A within 45 min; UV detection at 265 nm. Crude RNA products (trityl-off) were purified on a semipreparative Dionex DNAPac100 column (9 × 250 mm). Flow rate: 2 mL/min; gradient: Δ5−10% B in A within 20 min. Fractions containing RNA were loaded on a C18 SepPak cartridge (Waters/ Millipore), washed with 0.1−0.2 M $(Et_3NH)HCO_3$ and H_2O, and eluted with H_2O/CH_3CN (6/4). RNA fractions were lyophilized.

Oxidation of 2′-Methylseleno-Modified RNA. Oxidation was carried out by treating 2′-methylselenoguanosine-containing oligonucleotides (1.5 nmol) with 2 mM iodine in a solution of H_2O/CH_3CN/sym-collidine (65/10/1, v/v/v; 150 μL) for 5 min. Before analysis by ion-exchange column chromatography (Figure 3; Dionex DNAPac-100, conditions as above), the solution was extracted with $CHCl_3$/amyl alcohol (25/1, v/v; 50 μL) twice to remove excess iodine.

Reduction of 2′-Methylselenoxide-Modified RNA. Reduction of 2′-methylselenoxide containing oligonucleotides was achieved by treatment with DTT in water (1.5 nmol of RNA, 2 mM DTT in 150 μL of H_2O) for 5 min. The reaction mixture was directly analyzed by ion-exchange column chromatography (Figure 3; Dionex DNAPac-100, conditions as above).

Mass Spectrometry of 2′-Methylseleno Guanosine Containing RNAs. All experiments were performed on a *Finnigan* LCQ Advantage MAX ion trap instrumentation connected to an *Amersham* Ettan micro LC system. RNAs were analyzed in the negative-ion mode with a potential of −4 kV applied to the spray needle. LC: Sample (250 pmol of RNA dissolved in 20 μL of 20 mM EDTA solution; average injection volume: 10−20 μL); column (Amersham μRPC C2/C18; 2.1 × 100 mm) at 21 °C; flow rate: 100 μL/min; eluant A: 8.6 mM TEA, 100 mM 1,1,1,3,3,3-hexafluoro-2-propanol in H_2O (pH 8.0); eluant B: methanol; gradient: 0−100% B in A within 30 min; UV detection at 254 nm.

RNA Crystallization and Data Collection. For crystallization screening, RNAs (1 mM) were annealed in a buffer containing 50 mM potassium acetate (pH 6.9) and 5 mM $MgCl_2$ at 90 °C for 2 min and quickly cooled on ice. Crystals were grown by the hanging-drop vapor diffusion method using Crystal Screen, Crystal Screen 2, and Natrix kits (Hampton Research). The RNA and reservoir solutions were mixed in a 1:1 ratio (total volume 2 μL) and incubated at 4 and 20 °C for several days. Nonmodified and Se-modified RNAs were grown in parallel in the same wells. Crystals of dimensions 0.1 mm × 0.1 mm × 0.05 mm from the wells with Crystal Screen #15 solution (1.0 M Li_2SO_4, 0.1 M Na-citrate pH 5.6, 0.5 M $(NH_4)_2SO_4$) and Crystal Screen #9 solution (30% PEG4000 (w/v), 0.1 M Na-citrate pH 5.6, 0.2 M NH_4-aceteate) were frozen in liquid nitrogen without cryoprotection. Native and MAD data were collected at beamline X25 at the Brookhaven National Synchrotron Light Source (NSLS) from the crystals cooled at 100 K.

Structure Determination. X-ray data were processed with HKL2000 (HKL Research, VA) (Table 1). The "PEG4000" structure was determined using MAD selenium data. Heavy atom search and phasing was performed using SHARP,[47] including the solvent flattening procedure. Anomalous phasing power at peak was 1.08, and figure of

(47) de La Fortelle, E.; Bricogne, G. *Methods Enzymol.* **1997**, *276*, 472−494.

merit before/after solvent flattening was 0.45/0.87. Electron density maps were calculated using CCP4[48] up to 3.0 Å resolution limit. The RNA model was built manually using TURBO-FRODO (http://afmb.cnrs-mrs.fr/rubrique113.html) and refined with REFMAC up to 2.9 Å resolution limit using data collected from a similar crystal.[49] Alternatively, the structure can be solved by molecular replacement using MOLREP[48,50] and the native 16-mer RNA structure as a search model. The best MOLREP solution, however, places the RNA model to the wrong position within an infinite RNA helix. The model has to be shifted along the helical axis using the anomalous Se signal and the interruptions of the RNA backbone as beacons. The noncanonical G6•A27 and A11•G27 pairs were modeled using omit $2F_o - F_c$ and $F_o - F_c$ electron density maps calculated either without these purines or their bases. Due to limited resolution and rather poor quality of the omit maps, we attempted to build all major glycosidic conformations of these residues followed by refinement with REFMAC and analysis of the $2F_o - F_c$ and $F_o - F_c$ electron density maps. The G(syn)•A^+(anti) conformation showed the best refinement statistics and best fit to the maps and was chosen over the second best G(anti)•A^+(anti) conformation after analysis and comparison of the electron density maps calculated using data collected from a few independently grown crystals. Note that different molecules in the crystals may contain different conformations of the G•A pairs. The "Li_2SO_4" structure was solved by molecular replacement using MOLREP and the RNA model from the "PEG4000" structure and refined with REFMAC. Sulfate ions were added to the model based on analysis of $2F_o - F_c$ and $F_o - F_c$ electron density maps. All RNA residues were traced in the maps. Coordinates have been deposited in the Protein Data Bank (accession code 2H1M).

Acknowledgment. We gratefully acknowledge the Austrian Science Fund FWF (P17864) and the Tiroler Wissenschaftsfonds (GZ UNI-404/39) for funding and Kathrin Breuker (Cornell University and University of Innsbruck) for FT-ICR mass spectra. We are grateful to Dr. Dinshaw J. Patel for support (NIH GM073618), and Drs. L. Malinina and V. Kuryavyi for discussion. We thank M. Becker and the staff of beamline X25 (NSLS) for help in data collection.

Supporting Information Available: ^1H and ^{13}C NMR spectra of compounds **2**−**9**; ^1H NMR spectrum of compound **10**; tables of intermolecular distances for the 16-mer RNA duplex (PDF). This material is available free of charge via the Internet at http://pubs.acs.org.

JA0621400

(48) Collaborative Computational Project, Number 4. *Acta Crystallogr., D* **1994**, *50*, 760−763.
(49) Murshudov, G. N.; Vagin, A. A.; Dodson, E. J. *Acta Crystallogr., D* **1997**, *53*, 240−245.
(50) Vagin, A.; Teplyakov, A. *J. Appl. Crystallogr.* **1997**, *30*, 1022−1025.